



## Design, Synthesis, Characterization and Anticancer Evaluation of Novel Mixed Complexes Derived from 2-(1*H*-Benzimidazol-2-yl)aniline Schiff base and 2-Mercaptobenzimidazole or 2-Aminobenzothiazole



Fahad Mohammad Alminderej<sup>a</sup>, Lotfi Mohamed Aroua<sup>a, b\*</sup>

<sup>a</sup> Department of Chemistry, College of Science, Qassim University, King Abdulaziz Road, Al-Malida, 51452-P.O.Box: 6644, [Burraydah](#), Qassim, Kingdom of Saudi Arabia.

<sup>b</sup> Laboratory of Organic Structural Chemistry & Macromolecules, Department of Chemistry, Faculty of Sciences of Tunis, Tunis El-Manar University, El Manar I 2092, Tunis Tunisia.

### Abstract

Two Schiff base ligands ((benzimidazol-2-phenyl)iminomethyl)phenol (**HL1**) (**1**) and 2-(1-*H*-benzimidazol-2-yl)phenyl)imino)methyl) naphthol (**HL2**) (**2**) were synthesized via condensation of 2-(1-*H*-benzimidazol-2-yl)aniline and respectively salicylaldehyde or naphthylaldehyde. The synthesis of mixed complexes (**3**)-(6) was realized by reacting ligands **HL1** (**1**) and **HL2** (**2**), copper salt (CuCl<sub>2</sub>·2H<sub>2</sub>O) and respectively one equivalent of 2-mercaptobenzothiazole or 2-aminobenzothiazole. The ligands as well as the metal complexes have been identified with multiple spectroscopic techniques. The results data indicate that the copper is linked to ligands via deprotonated phenolic oxygen atom, nitrogen or sulphur atom of co-ligands and the coordination was realized through the azomethine group. X-ray powder diffraction analysis of complexes suggests that they possess monoclinic structure for complexes (**3**) and (**4**), while complex (**5**) has orthorhombic structure and rhombohedral structure for complex (**6**). The *in vitro* anticancer activities of the different complexes were evaluated and the results revealed an important cytotoxicity of complex (**6**) against lung human cancer A-549 and very good selectivity with 12.4 values of inhibitory concentration IC 50. The best result was described with complex (**4**) and present high activities on both A-549 and Caco-2 indicating good selectivity on lung human cancer A-549 and moderate selectivity on colorectal cell line Caco-2 with 10.9 and 15.7 respectively of IC 50.

**Keys words:** Copper mixed complex, Schiff base, anticancer evaluation, 2-(1-*H*-Benzimidazol-2-yl) aniline, 2-aminobenzothiazole, 2-mercaptobenzothiazole

### Introduction

Benzimidazole scaffolds is an excellent structure that displays great physiological and therapeutic activity. In past years, the study reporting the influence of systems containing benzimidazole moiety was considerably increased and incorporated vast activities including antimicrobial [1,2], antihelminthic [3], antithrombotic, antiplatelet and anticoagulant [4], anti-inflammatory [5,6], antiulcer [7], antifungal and acetylcholinesterase [8], antiprotozoal and antitubercular [9], antileishmanial [10], antimycobacterial [11], antiviral [12], anti-HIV [13] and antitumour [14].

In addition, benzimidazole target was described as inhibitors of the hepatitis C virus [15], indoleamine 2,3-dioxygenase-1 (IDO1) inhibitors from structure-based virtual screening to *in Vivo* pharmacodynamic activity [16], anti-hypertensive agent [17], Zika Virus

Inhibitors [18], *in vitro* alpha-glucosidase inhibitory [19], NOD2 antagonists [20], antiglycation and antioxidant [21] and antileukemic agents [22]. Surineni G. et al. considered that the benzimidazole core were used with excellent efficiency for the treatment of tuberculosis [23]. Recently, benzimidazole scaffolds were reported as anti-cancer agents in a diverse review [24,25].

As a consequence, diverse drugs originated from benzimidazole system have been introduced into the market cover albendazole (antimicrobial), omeprazole (Anti-ulcer), Bendamustine (Anti-tumor), Envirodine (Anti-viral), Candesartan (Anti-hypertensive) and Benoxaprofen Analog (Anti-inflammatory) [26].

On the other hand, benzimidazoles nucleus gained diverse applications, particularly, they extensively

\*Corresponding author e-mail: [aroua.lotfi@yahoo.com](mailto:aroua.lotfi@yahoo.com), [lm.aroua@qu.edu.sa](mailto:lm.aroua@qu.edu.sa) (Lotfi Mohamed Aroua,)

Receive Date: 31 January 2021, Revise Date: 11 February 2021, Accept Date: 22 March 2021

DOI: 10.21608/EJCHEM.2021.60640.3305

©2021 National Information and Documentation Center (NIDOC)

used as ligands in the development of the metal complex. Among, a diverse of benzimidazole complexes were reviewed and manifested several significant biological activities covering antibacterial [27], antifungal [28], antioxidant activity against DPPH and antidiabetic activity against  $\alpha$ -amylase [29], antiameobic [30], Potent inhibition of protein tyrosine phosphatases [31] and antimalarial [32].

Furthermore, the Schiff base elaborated from 2-(1*H*-benzimidazol-2-yl)aniline and 2-hydroxysalicylaldehyde was recognized as an essential precursor leading the synthesis of diversely metal complexes owning therapeutic potential including antibacterial [33], analgesic and anti-inflammatory [34], and anticancer [35]. The architecture complex involving 2-((methyl-benzimidazol-2-phenyl) imino methyl) phenol have been also a multitude of applications as chemosensors [36-38].

Moreover, 2-(1*H*-benzimidazol-2-yl) aniline was reviewed as important of targeted owning a broad range of applications in different fields. In particular, a complex established with 2-hydroxynaphthaldehyde is well described in medicinal chemistry as anticancer [39].

In recent years, cancerous disease has been regarded as one of the public health problems in many countries, and research in this area has thus greatly increased. A variety of drugs was introduced in the market covering Paclitaxel known as Taxol used to treat a number of cancer including ovarian cancer, breast cancer, lung cancer, Kaposi sarcoma, cervical cancer and pancreatic cancer [40]. Docetaxel (known as Taxotere) is a chemotherapy medication used against a number of cancers. This includes breast cancer, head and neck cancer, stomach cancer, prostate cancer and non-small-cell lung cancer [41]. Bevacizumab, (Avastin) is a drug employed against colon cancer, lung cancer, glioblastoma, and renal-cell carcinoma [42].

In continuation to develop and discover a novel molecular architecture possessing biological activities [43-48], we report the synthesis and anti-cancer evaluation of new mixed metal copper complexes derived from 2-aminomethylbenzothiazole, 2-aminomethylbenzothiazole and Schiff base of 2-(1*H*-benzimidazol-2-yl)aniline as ligand.

## Experimental

### Material and Methods

Electronic absorption spectra were registered using a UV-2102 PC Shimadzu spectrophotometer in the 200-900 nm wavelength range using DMF as a solvent. The FT-IR spectra was achieved from a Thermo-Nicolet-6700 FT-IR spectrometer with performing a KBr disc procedure in the range 400-4000  $\text{cm}^{-1}$ . TGA and DTA studies were realized

using Shimadzu DTG-60 (10°C/min heating rate). The mean sample weight was 10 mg  $\alpha$ - $\text{Al}_2\text{O}_3$  as reference. X-ray powder diffraction patterns was obtained on Philips XRD diffractometer Model PW 1710 control unit with anode spacing Cu  $K\alpha$  ( $\lambda = 1.54180 \text{ \AA}$ ), 40 kV and 30 mA for optics. All reagents applied to synthesize different complexes were commercially available without purification. 2-(1*H*-benzimidazol-2-yl) aniline, 2-aminobenzthiazole and 2-mercaptobenzothiazole were purchased from Sigma-Aldrich. The high-Resolution mass spectra were acquired on Mass Spectrometer type AccuTOF LC-Plus from JEOL (Japan). Mass spectra of different complexes are recorded in positive mode using DART-TOF-MS. Two to five of the most intense fragment ions resulting from cleavage possible from the compounds detected were chosen and analyzed. The  $^1\text{H}$  and  $^{13}\text{C}$ -NMR spectra were performed on Bruker NMR at 400 and 100 MHz respectively. The chemical shifts were determined using TMS as an internal standard reference in  $\text{DMSO-}d_6$  as the solvent.

### Preparation of ((benzimidazol-2-phenyl)imino methyl)phenol (HL1) (1)

This protocol was realized according the literature condition [37]. A solution of 2-(1*H*-benzimidazol-2-yl)aniline (1.05 g, 5mmol) in 35 mL of anhydrous methanol was heated gradually at 65 °C for 30min. Then, a solution of salicylaldehyde (0.67 g, 5.5 mmol) dissolved in 10 mL of anhydrous methanol was added and the mixture was refluxed for 4h. After the end of the reaction, the mixture was cooled and the solvent was removed under reduced pressure. The residue was purified by recrystallization in ethanol to give as a pale yellow crystal powder. Described data agreed with that reported.

Yield: 82%., Mp = 122-124,  $^1\text{H}$  NMR (400MHz,  $\text{DMSO-}d_6$ ),  $\delta$ (ppm): 10.18 (s,1H), 7.94 (s,1H), 7.64 (d, 1H), 7.15 (m, 7H), 6.89 (dd, 2H), 6.80 (t, 1H) , 6.65 (m, 2H).  $^{13}\text{C}$  NMR (100 MHz,  $\text{DMSO-}d_6$ )  $\delta$ (ppm): 154.77, 147.81, 144.35, 143.97, 133.36, 131.98, 130.46, 126.95, 126.57, 125.05, 122.60, 122.43, 119.73, 119.06, 118.29, 116.29, 115.24, 112.03, 110.68, 63.50. IR (KBr pellets,  $\text{cm}^{-1}$ ): 3398.67 (O-H). 3252.22 (N-H), 1651 (C=C), 1664 (C=N), 1298.83 (C-N). Elemental analysis For  $\text{C}_{20}\text{H}_{16}\text{N}_3\text{O}$  calcd.: C, 76.58; H, 4.98; N, 13.32%. Found: C, 76.66; H, 4.82; N, 13.41%. HRMS for  $\text{C}_{20}\text{H}_{16}\text{N}_3\text{O}$  calcd.: 314.1288, Found: 314.1289.

### Preparation of 2-(1*H*-benzimidazol-2-yl)phenyl imino)methyl) naphthol (HL2) (2)

The ligand (HL2) (2) was prepared via the general procedure reported in the literature [40]. To a solution of 2-(1*H*-benzimidazol-2-yl)aniline (1.05 g, 5 mmol) dissolved in 50 mL of ethanol, was added a

solution of 2-hydroxy-1-naphthaldehyde (0.86 g, 5 mmol) dissolved in 20 mL of ethanol and three drop of acetic acid were added. Then, the mixture left at reflux for 5 h. At the end of the reaction, the volume was reduced. Diethyl ether was added and the solution was left in refrigerator. Light yellow crystals collected, filtered, washed with diethyl ether and dried. Described data agreed with that reported.

Yield: 75%. IR (KBr pellets,  $\text{cm}^{-1}$ ):  $\nu_{\text{C=N}}$ : 1634.  $^1\text{H}$  NMR ( $\text{CDCl}_3$ , 400 MHz),  $\delta$  (ppm): 14.43 (s, 1H, OH), 9.41 (s, 1H, CH=N), 7.95 (d, 1H, Ar-H), 7.88 (s, 1H, Ar-H), 7.78 (d, 1H, Ar-H), 7.68 (m, 1H, Ar-H), 7.53 (s, 1H, Ar-H), 7.50 (s, 1H, Ar-H), 7.45 (s, 1H, Ar-H), 7.40 (s, 1H, Ar-H), 7.34 (m, 1H, Ar-H), 7.01 (d, 1H, Ar-H).  $^{13}\text{C}$  NMR ( $\text{CDCl}_3$ , 75. MHz),  $\delta$  (ppm): 166.31, 158.85, 136.14, 132.35, 131.47, 129.23, 128.08, 127.57, 126.66, 123.65, 123.01, 120.54, 119.84, 119.54, 119.17, 109.75. Elemental analysis for  $\text{C}_{25}\text{H}_{19}\text{N}_3\text{O}$ , Calcd.: C, 79.56; H, 5.08; N, 11.11%. Found : C, 79.78; H, 4.99; N, 10.99%.

#### Preparation of mixed complex (3) and (4).

To a solution of ((benzimidazol-2-phenyl)imino methyl)phenol (0.43 g, 1.377 mmol) in 10 mL of ethanol was added a solution of copper chloride dehydrate (0.234g, 1.377 mmol) in 10 mL of ethanol. The reaction mixture was stirred at room temperature for 30 mn and respectively a solution of 2-mercaptobenzothiazole (0.23g, 1.377 mmol) or 2-aminobenzothiazole (0.20g, 1.377 mmol) in 10mL of ethanol was added. Then, the reaction mixture was refluxed for 4 h. The progress of reaction was monitored with TLC (DMF/ethanol: 20/80). At the end of the reaction, the mixture was cooled, filtered, washed with ethanol and then with small portion of DMF.

#### Complex (3)

Yield:78%, Mp: 165°C, UV-Vis (DMF);  $\lambda_{\text{max}}$  [nm]: 272; 290, 298, 302, 331, 345. IR (KBr,  $\nu$  / $\text{cm}^{-1}$ ): = 3226 (m), 2628 (m), 1631 (m), 1606 (s), 1531 (s), 1489(m), 1462 (s), 1362 (m), 131 (s), 1272 (m), 1237 (m), 1183 (m), 1156 (m), 1080 (m), 1051 (s), 1005(m), 874 (m), 792 (m), 757 (m), 742 (m), 644 (m), 606 (m), 562 (m), 535 (m), 509 (m),. 455 (m), 433 (m). HRMS (DART-TOF-MS, positive mode)  $m/z$ = 624.41257, 564.36313, 520.33287, 476.31261, 446.26794, 432.27610, 388.26014, 363.03582, 332.96718, 314.13189, 300.20138, 269.01905, 250.13027, 229.04522, 210.10099, 136.04938.

#### Complex (4)

Yield: 75%, 229, UV-Vis (DMF);  $\lambda_{\text{max}}$  [nm]: 292; 417. IR (KBr,  $\nu$  / $\text{cm}^{-1}$ ): = 3181 (m), 1606 (m), 1577 (m), 1530 (s), 1461 (s), 1441(m), 1383 (s), 1321 (m), 1280 (s), 1225 (m), 1183 (m), 1141 (m), 1094 (m), 966 (m), 928 (s), 861(m), 823 (m), 795 (m), 755 (m), 742 (m), 701 (m), 644 (m), 606 (m), 580 (s), 561(m),

532 (m), 510 (m), 455 (m). 433 (m). HRMS (DART-TOF-MS, positive mode)  $m/z$ = 521.25317, 477.23183, 429.20721, 373.13017, 345.16007, 301.06311, 264.12219, 229.04528, 151,03002.

#### Preparation of mixed complex (5) and (6)

To a solution of 2-(1-*H*-benzimidazol-2-yl)phenyl imino)methyl) naphthol (0.5 g, 1.377 mmol) in 10 mL of ethanol was added a solution of copper chloride dehydrate (0.234g, 1.377 mmol) in 10 mL of ethanol. The reaction mixture was stirred at room temperature for 30 mn and respectively a solution of 2-mercaptobenzothiazole (0.23g, 1.377 mmol) or 2-aminobenzothiazole (0.20g, 1.377 mmol) in 10mL of ethanol was added. Then, the reaction mixture was heated under reflux for 4 h. The progress of reaction was controlled with TLC (DMF/ethanol: 20/80). At the end of the reaction, the mixture was cooled, filtered , washed with ethanol and then with small portion of DMF.

#### Complex (5)

Yield: 82%, Mp: 328°C, UV-Vis (DMF);  $\lambda_{\text{max}}$  [nm]: 273; 292, 302, 326, 432. IR (KBr,  $\nu$  / $\text{cm}^{-1}$ ): = 3112 (m), 3060 (m), 1600 (m), 1567 (s), 1529 (s), 1487(m), 1443 (s), 1362 (m), 1241 (s), 1185 (m), 1149 (m), 1079 (m), 1006 (m), 865 (m), 831 (s), 747(m), 722 (m), 696 (m), 604 (m). 559 (m), 526 (m), 505 (m), 455 (m), 427 (m). HRMS (DART-TOF-MS, positive mode)  $m/z$ =: 314.12871, 279.18635, 236.11896, 220.08488, 183.01010, 151.05363.

#### Complex (6)

Yield: 85%, Mp: 267°C, UV-Vis (DMF);  $\lambda_{\text{max}}$  [nm]: 258; 272, 292, 302, 324, 432. IR (KBr,  $\nu$  / $\text{cm}^{-1}$ ): = 3117 (m), 3361 (m), 3267 (m), 1598 (s), 1566 (s), 1529(m), 1486 (s), 1443 (m), 1421 (s), 1291 (m), 1185 (m), 1148 (m), 1092 (m), 1050 (m), 975 (s), 863(m), 831 (m), 739 (m), 695 (m). 648 (m), 559 (m), 503 (m), 455 (m), 427 (m). HRMS (DART-TOF-MS, positive mode)  $m/z$ =: 436.33991, 380.27461, 352.26318, 324.22095, 296.19604, 268.15132, 235.23617, 219.24212, 180.14166, 151.03025, 102.08938.

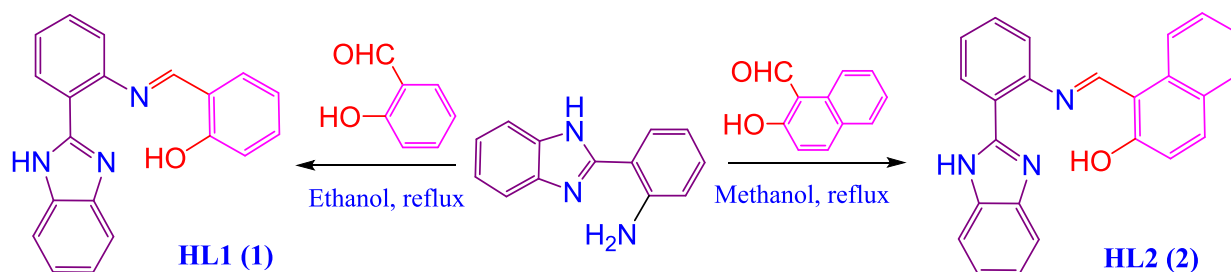
#### *In-vitro* anticancer activities

The cytotoxicity activities toward one lung human cancer (A-549), two human colorectal cancer (Caco-2 and HT-29), and normal retina (RPE-1) cell lines were evaluated using the 3-[4,5-dimethyl-2-thiazolyl]-2,5-diphenyl-2*H*-tetrazolium bromide (MTT) assay [49-51]. These different cancer cell lines were purchased from ATCC (Rockville, MD, USA). The cytotoxicity test was realized from National Research Centre, Cairo 12311, Egypt.

The cells were cultivated in a 96-well sterile microplate ( $5 \times 10^4$  cells per well) at 37 °C in Roswell Park Memorial Institute medium (RPMI-1640)

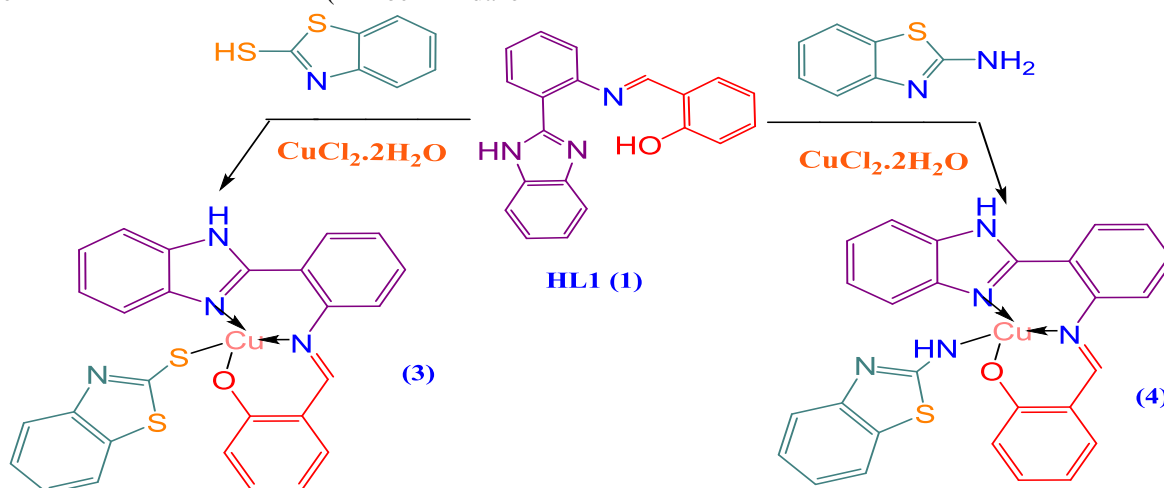
supplemented with 10% heat-inactivated fetal bovine serum (FBS) and 100 U/mL of both penicillin and streptomycin in a 5% CO<sub>2</sub> humidified atmosphere. After 24 hours, the media were removed and a fresh serum-free medium (90 uL/well) was added together with 10 uL of series of compounds or doxorubicin (positive control) concentrations in DMSO for 48 hours. Then, media were removed, MTT (40 uL of 2.5 mg/mL) was added to each well and incubated for 4 hours. 200 uL of DMSO was added to solubilized the formazan dye crystals (purple color). Using a SpectraMax Paradigm Multi-Modemicroplate reader, the absorbance was measured at 590 nm. Each experiment was repeated on three different days and conducted in triplicate. The relative cell cytotoxicity was measured according to the following equation:

$$\% \text{ cytotoxicity} = (1 - A_s/A_b) * 100$$



**Scheme 1:** Synthesis of Ligands **HL1 (1)** and **HL2 (2)**

The synthesis of mixed complexes (**3**) and (**4**) was realized by reacting one equivalent ethanolic solution of **HL1 (1)**, one equivalent of copper salt (CuCl<sub>2</sub>·2H<sub>2</sub>O) in the same solvent and respectively one equivalent of 2-mercaptobenzothiazole or 2-aminobenzothiazole (Scheme 2). The same protocol was adopted to the synthesis of complexes (**5**) and (**6**) from



**Scheme 2:** Structure of mixed complexes derived from ((benzimidazol-2-phenyl)iminomethyl)phenol (**HL1 (1)**)

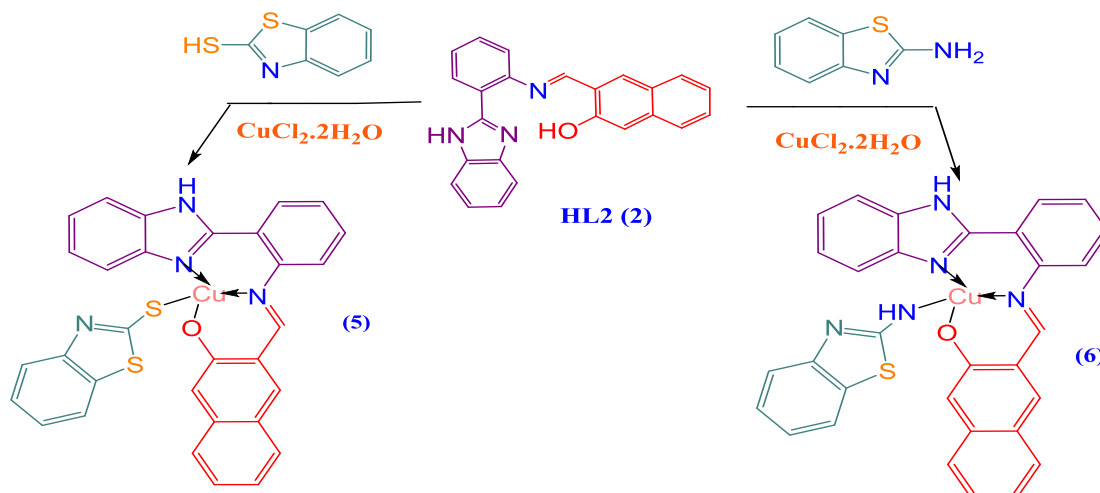
Where; A<sub>s</sub>: Absorbance of each sample and A<sub>b</sub>: blank Absorbance. The probit analysis using the SPSS software program (version 20, SPSS Inc., Chicago, IL, USA) was used to determine each IC<sub>50</sub>.

## Results and Discussion

### Chemistry

Our study started with the synthesis of ligands ((benzimidazol-2-phenyl)iminomethyl)phenol (**HL1 (1)**) and 2-(1-*H*-benzimidazol-2-yl)phenyl(imino)methyl naphthol (**HL2 (2)**) via condensation of 2-(1-*H*-Benzimidazol-2-yl)aniline and respectively salicylaldehyde or naphthylaldehyde according to the literature conditions [37, 40] and following the Scheme 1

yl)phenyl(imino)methyl) naphthol **HL2 (2)** (Scheme 3). All new obtained complexes were fully characterized by spectroscopic data of high resolution Mass spectrometry (HRMS), UV-Visible electronic absorption, FT-IR, thermal analysis and X-ray powder diffraction. Analytical data was resumed in Table 1



**Scheme 3:** Structure of mixed complexes derived from 2-(1-*H*-benzimidazol-2-yl)phenyl)imino) methyl naphthol (HL2) (2)

**Table 1:** Analytical data of mixed synthesized complexes

Entry	Complex	Colour	Empirical formula	Yield (%)	Mp(°C)
1	3	Green	$\text{C}_{27}\text{H}_{18}\text{N}_4\text{OS}_2\text{Cu}$	78	165-167
2	4	Dark Green	$\text{C}_{27}\text{H}_{19}\text{N}_5\text{OSC}_2$	75	229-230
3	5	Brown	$\text{C}_{31}\text{H}_{20}\text{N}_4\text{OS}_2\text{Cu}$	82	328-330
4	6	Dark Brown	$\text{C}_{31}\text{H}_{21}\text{CuN}_5\text{OS}$	85	335-337

Mass spectra of complex (3) represented in Figure 1, manifest that the structure is tetrahedral. This structure was accomplished essentially by molecular ion peak situated at  $m/z = 564.36313$  (calcd. 564,01157) attributed to  $[\text{M}+\text{Na}]^+$ . Also, the spectra display the presence of another peak at  $m/z = 446.26794$  (calcd 446,11624) assigned to ligand HL1 (1) linked with copper and but-2-enamine. The peak at  $m/z = 432.27610$  (calcd. 432.10059) was assigned

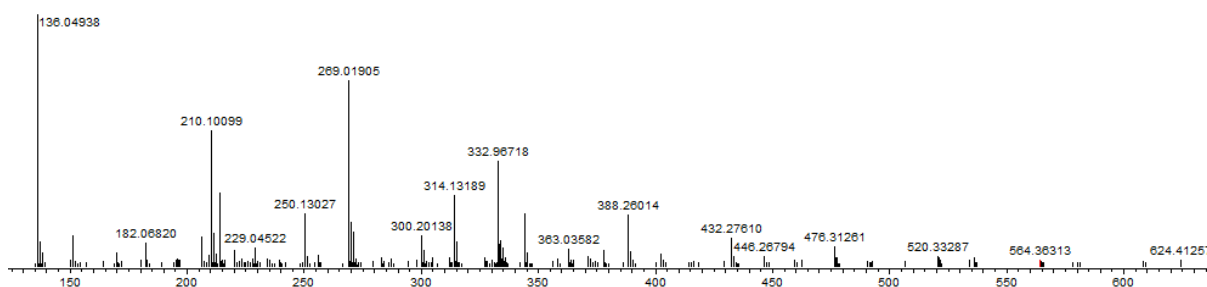


**Figure 1:** Mass Spectra of complex (3)

The mass spectrum of complex (4) presented in Figure 2, manifest the absence of molecular ion. The structure was also confirmed by: the first fragment at  $m/z = 477.23183$  (calcd. 477,06791) corresponding to ligand HL1(1) linked to copper ion and 4,5-dihydrothiazol-2-amine. The fragment at  $m/z = 429.20721$  (calcd. 429,06791) associated to the benzimidazolphenyliminopropanol motif connected

to ligand HL1 (1) connected with copper and prop-2-enamine. The fragment at  $m/z = 314.13189$  (calcd. 314.12879) corresponding to ligand HL1<sup>+</sup>. The basic fragment at  $m/z = 136.04938$  (calcd. 136,07569) was associated to tetrahydrobenzooxazin-1-ium. These data confirm also that the copper atom is linked with Ligand HL1 (1) and 2-mercaptobenzothiazole and coordinated with the two azomethine group of ligands HL1 (1) (Scheme 2).

to copper metal and 4,5-dihydrothiazol-2-amine. The peak at  $m/z = 373.13017$  (calcd. 373,09584) is connected to benzimidazolphenyliminopropanol to copper ion and methanedi-amine. Another peak at  $m/z = 345.16007$  (calcd. 345,07711) was attributed to benzimidazolphenyl aminopropanol attached to copper ion and ammonia molecule. The spectra it reveals also a peak located at  $m/z = 301.06311$  (calcd.

301,02709) assigned to benzoimidazobuta-1,3-dienamino acrylaldehyde linked with copper ion. The fragment at  $m/z=229.04528$  (calcd. 229,02709) was qualified to 3-amino-3-vinylaminoallylamino acryl aldehyde connected to copper ion. The basic peak at  $m/z = 151.03002$  (calcd. 151,03245) was allowed to benzothiazol-2-aminium. These results suggest

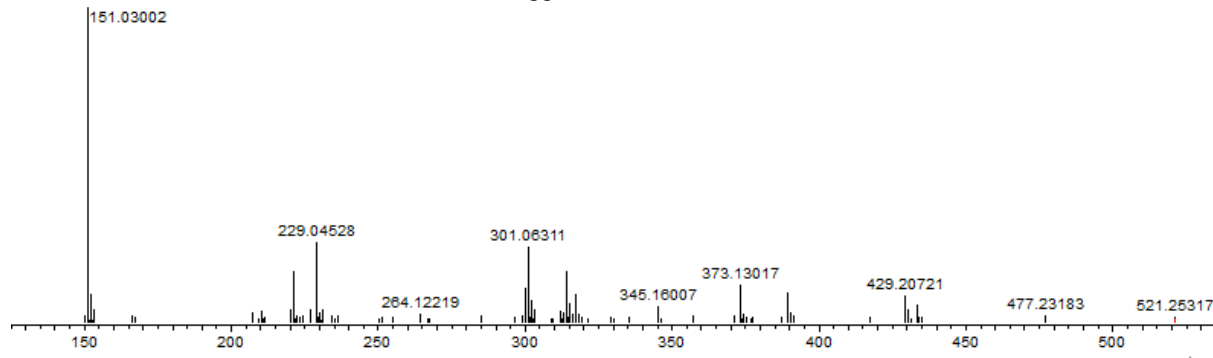


**Figure 2:** Mass Spectra of complex (4)

The mass spectra of complex (5) observed in Figure 3, exhibited the absence of a molecular peak. The structure was proved essentially by ion peak located at  $m/z = 314.12871$  (calcd. 314.12871) corresponding to benzoimidazolphenylamino-2-methylpropanal linked with copper. The peak situated at  $m/z=279.18635$  (calcd. 279.04329) attributed to benzoimidazol ethylaminopropanal connected with copper. Furthermore, the spectra manifest the presence of another peak at  $m/z=236.11898$  (calcd. 236,02435) assigned to benzoimidazoethyl methanimine connected with copper metal. The basic

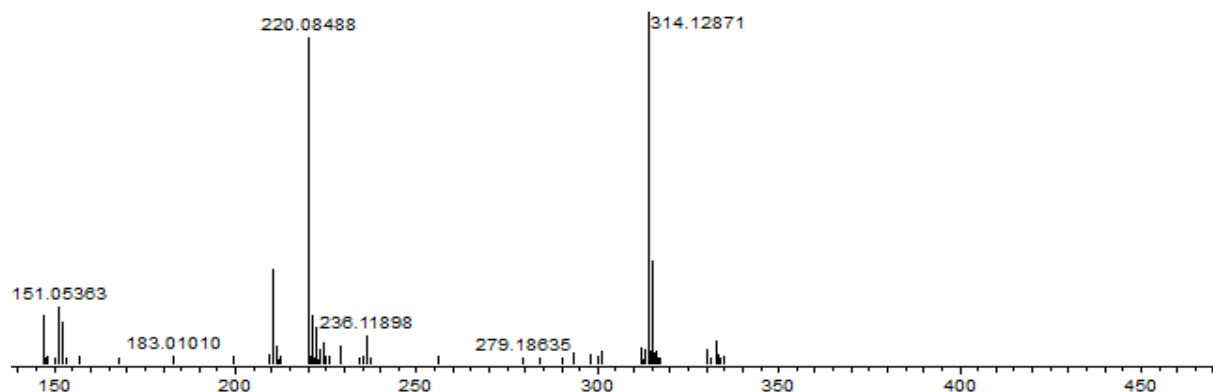


**Figure 3:** Mass Spectra of complex (5)

Regarding the mass spectra of complex (6), illustrated in Figure 4, reveal the nonexistence of molecular peak. The structure was proved essentially by ion peak situated at  $m/z = 436.33991$  (calcd. 436,04136) associated to benzoimidazolphenyliminomethylphenol linked with copper and methanimidothioic acid. The peak located at  $m/z=235.23617$  (calcd. 235,11043) attributed to N-cyclohexylmethanediamine connected with copper

tetrahedral structure of copper and it is linked with ligand HLL (1) via deprotonated phenolic oxygen atom and 2-aminobenzothiazole via nitrogen atom. The coordination of the copper has been provided by the amino groups of both azomethine groups (Scheme 2).

fragment at  $m/z=200,08488$  (calcd. 200,04950) was associated to N-propylcyclohexa-1,5-dienamine linked to copper metal. The peak at  $m/z = 151.05363$  (calcd. 151,03245) assigned to benzothiazol-2-aminium.

These results prove the formation of the complex and posses tetrahedral structure. The copper is linked to ligand via hydroxyl group and mercapto group of co-ligand 2-mercaptobenzothiazole. The coordination of copper metal was established with both the azomethine group of ligand (Scheme 3).

and ethylamine. Furthermore, the spectra manifest the presence of another peak at  $m/z=219.24212$  (calcd. 219,07913) assigned to N-cyclohexylmethanediamine connected with copper metal and methanimine. The peak at  $m/z = 151.03025$  (calcd. 151,03245) assigned to benzothiazol-2-aminium. The basic fragment at  $m/z=102,08938$  (calcd. 102,12773) was associated to hexanaminium.

This information, in the case of complex (6), affirms that the metal is associated first to the ligand by the hydroxyl group and with amino group of co-

ligand 2-aminobenzothiazole. The coordination of copper was assured with both azomethine group of principle ligand HL2 (2) (Scheme 3).

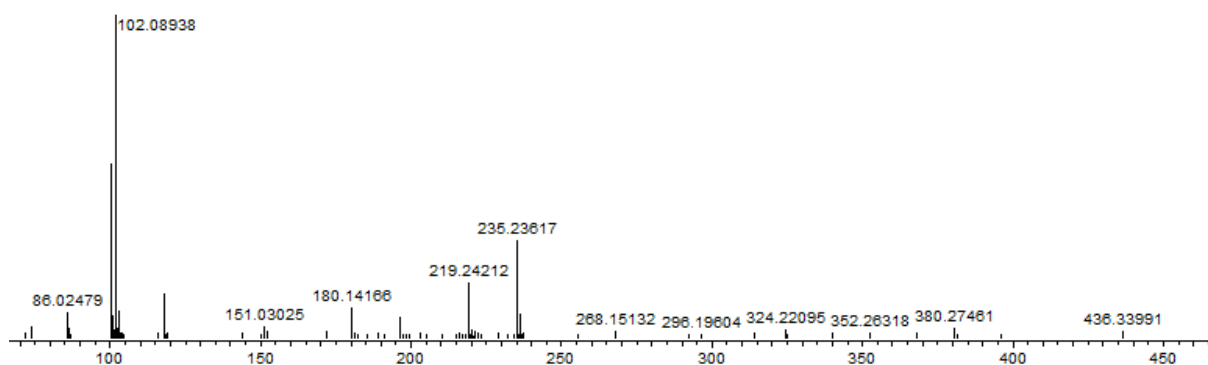


**Figure 4:** Mass Spectra of complex (6)

These results manifest, for all complexes that the chlorine atoms are a good leaving groups and they have undergone the nucleophilic attacks via hydroxyl group of ligands as well as mercapto or amino group of both co-ligand respectively 2-mercaptobenzo thiazole or 2-aminobenzothiazole.

The IR results of free ligands and its copper complexes were summarized in Table 2. The ligand HL1 (1) display the presence of broad and strong band at 3398  $\text{cm}^{-1}$  attributed to the stretching vibration of the phenolic hydroxyl group. In the case of complexes (3) and (4), the spectra reveal the absence of the OH stretching vibration which corresponding to the deprotonation of the hydroxyl group in the formation processes of the complex.

The spectra of HL1 (1) present another band at 3252  $\text{cm}^{-1}$  assigned to the  $\nu(\text{NH})$  group of benzimidazole moiety. This band was shifted at a lower frequency in the complex (3) and (4) and located respectively at 3226 and 3181  $\text{cm}^{-1}$ . Eventually, the spectra of HL1 (1) exhibited the presence of a strong band situated at 1664  $\text{cm}^{-1}$  assigned to azomethine group. This band which deviates in the complexes (3) and (4) and shifted to lower frequencies (1631, 1606  $\text{cm}^{-1}$ ) that is in a good

agreement with the previously reported data [52, 53]. This mode of chelation is supported by the appearance of new bands in the 455  $\text{cm}^{-1}$  and (561-562)  $\text{cm}^{-1}$  attributed to  $\nu(\text{O}\rightarrow\text{M})$  and  $\nu(\text{N}\rightarrow\text{M})$  and respectively (Table 2). These bands were absent in the spectra of the ligand, thus confirming the participation of oxygen, nitrogen and sulfur atoms in the coordination.

Consulting the Table 2, the ligand HL2 (2) manifest also the presence of strong band at 3385  $\text{cm}^{-1}$  corresponding to  $\nu(\text{OH})$  of phenolic group. This band disappeared completely in the case of complex (5) and (6) indicating the coordination of oxygen with copper atom. The ligand HL2 (2) reveal the presence of another band at 1634  $\text{cm}^{-1}$  associated to azomethine function. This band is still observed in the complexes (5) and (6), but it is shifted to lower frequencies at 1600 and 1598  $\text{cm}^{-1}$  respectively involving the coordination of ligand HL2 (2) with copper metal via azomethine group. Furthermore, the coordination of the ligand with the metal ions was manifested by the appearance of new bands at the range of 559  $\text{cm}^{-1}$ , and 455  $\text{cm}^{-1}$  respectively assigned to metal-nitrogen (M-N) and (M-O) vibrations respectively (Table 2) [54,55].

**Table 2:** The vibrational assignment wavenumbers in  $\text{cm}^{-1}$  of ligands and mixed complexes

complex	$\nu(\text{OH})$	$\nu(\text{N-H})_{\text{benzim}}$	$\nu(\text{C=N})$	$\nu(\text{M-O})$	$\nu(\text{M-N})$
HL1 (1)	3398	3252	1664	-	-
HL2 (2)	3385	3235	1634	-	-
Complex (3)	-	3226	1631	455	562
Complex (4)	-	3181	1606	455	561
Complex (5)	-	3112	1600	455	559
Complex (6)	-	3117	1598	455	559

The electronic spectra of ligands and mixed metal complexes were realized in DMF at room temperature. The results of the electronic spectral

data of the Schiff base and their complexes are given in Table 3. The Free ligand HL1 (1) present first band absorption at 282 nm attributed to  $n\rightarrow\pi^*$  transition associated with azomethine group (-

CH=N). This band is still observed in the complexes (3) and complex (4), but it is shifted to lower frequencies respectively at 290 and 292 nm [55]. The spectra of complex (3) display also, two bands at 302 and 331 nm relatively to  $\pi \rightarrow \pi^*$  transition and another band at 345 nm associated with ligand-to-metal charge transfer transition (phenoxy-to-copper) [40]. The complex (4) manifests a band at 388 nm assigned to  $\pi \rightarrow \pi^*$  transition and also a band at 345 nm attributable to ligand-to-metal charge transfer transition (phenoxy-to-copper). The complexes (5) and (6) reveal the presence a band located respectively at 326 and 324 nm corresponding to  $\pi \rightarrow \pi^*$  transition of azomethine group and a transition attributed to ligand-to-metal charge transfer transition (phenoxy-to-copper) located at 432 nm.

The investigation of thermal decomposition of several complexes was performed at room temperature. The thermograph degradation of the hybrid complex (3) reveals principally two endothermic decomposition stages. The first endothermic stage at 221-405°C is responsible for the

desorption of ligand HL1 (1) with mass loss amounting to 57.71% (calcd. 57.61). The second exothermic step in the range of 475-577 °C is assigned to the elimination copper oxide molecule with a mass loss amounting to 13.31 % (calcd. 13.47 %). The thermal decomposition of complex (4) engender essentially an endothermic stage at 250-385 °C with a mass loss 56.54% (calcd. 56.68) corresponding to the detachment of ligand HL1 (1). Moreover, complex (5) exhibited two endothermic decomposition stages. The first step at 245-306°C associated for the degradation of benzene ring with mass loss amounting to 13.67% (calcd. 13.17). The second consist to desorption of naphthalen-2-ol at 327-395°C with mass loss amounting to 24.79% (calcd. 24.32). Two endothermic stages described the thermal analysis of complex (6). In fact, located at 236-307°C, first endothermic stage assigned to exclusion of benzothiazole with mass loss amounting to 23.90% (calcd. 23.47). Second stage manifests also the elimination of 3-methylnaphthalen-2-ol with mass loss to 27.59% (calcd. 27.50).

**Table 3:** The electronic data of free ligands and their mixed complexes

Compound	$\lambda_{\max}$ [nm]	$\nu(\text{Cm}^{-1})$	Assignment
Ligand HL1 (1)	282	35460	$n \rightarrow \pi^*$
	290	34482	$n \rightarrow \pi^*(\text{CH}=\text{N})$
	302	33112	
Complex (3)	331	30211	$\pi \rightarrow \pi^*(\text{CH}=\text{N})$
	345	28985	${}^2\text{B}_{1g} \rightarrow {}^2\text{A}_{1g}$
Complex (4)	292	34246	$n \rightarrow \pi^*(\text{CH}=\text{N})$
	388	25773	$\pi \rightarrow \pi^*(\text{CH}=\text{N})$
	417	23980	${}^2\text{B}_{1g} \rightarrow {}^2\text{A}_{1g}$
Ligand HL2 (2)	310	30581	$\pi \rightarrow \pi^*$
	292	34246	
	302	33112	$n \rightarrow \pi^*(\text{CH}=\text{N})$
Complex (5)	326	30674	$\pi \rightarrow \pi^*(\text{CH}=\text{N})$
	432	23148	${}^2\text{B}_{1g} \rightarrow {}^2\text{A}_{1g}$
Complex (6)	292	34246	
	302	33112	$n \rightarrow \pi^*(\text{CH}=\text{N})$
	324	30864	$\pi \rightarrow \pi^*(\text{CH}=\text{N})$
	432	23148	${}^2\text{B}_{1g} \rightarrow {}^2\text{A}_{1g}$

Single crystals of different hybrid complexes (3)-(6) with different solvents covering DMF, ethyl alcohol, chloroform is failed and they were identified by XRD powder diffraction. X-ray powder diffraction study of metal hybrid complexes was provided to determine the type of crystal system, lattice parameters,  $2\theta$  range and crystallinity size, and the cell volume. From the indexed data, the unit cell parameters were also calculated and are listed in Table 4. The powder XRD patterns of synthesized

compounds possess monoclinic structure for complexes (3) and (4), while complex (5) has orthorhombic structure and Rhombohedral structure for complex (6). The crystal structures of similar type of samples were reported as monoclinic and orthorhombic [56, 57]. Moreover, using the diffraction data, the mean crystallite sizes of the complexes,  $D$ , were determined according to the Scherrer equation ( $D = K \lambda / \beta \cos \theta$ ), where  $K$  is the shape factor and  $\lambda$  is X-ray wavelength (1.5406 Å),  $\beta$  is Bragg diffraction angle,

and  $\theta$  is the full width at half maximum of the diffraction peak) [58,59]. Biology

#### In vitro anticancer activities

The cytotoxicity of the synthetic metal complexes (3)–(6), against lung human cancer A-549 (served as models of alveolar type II pulmonary epithelium), human colorectal cancer Caco-2 (heterogenous human epithelial colorectal adenocarcinoma cells) and colon cancer cell line HT-29 and normal retina RPE-1 cell lines were assessed using the 3-[4,5-

dimethyl-2-thiazolyl)-2,5-diphenyl-2H-tetrazolium bromide (MTT) assay.

The results of the different analyses were collected in Table 5-7. As depicted in Table 5, for all human cells, the percentage cytotoxicity of the complexes (at 100  $\mu$ M) reveals that the complexes (4) and (6) have the most important percentage of cytotoxicity. Complexes (3) and (5) indeed exhibit moderate cytotoxicity. This result may be due to the presence of the amino group of co-ligand 2-aminobenzothiazole.

**Table 4:** X-ray powder diffraction crystal data of complexes: Lattice constant, inter axial angle, Crystal system, unit cell volume,  $2\theta$  range and crystallinity size of different metal complex

Parameters		Complex (3)	Complex (4)	Complex (5)	Complex (6)
Empirical formula		$C_{27}H_{18}N_4OS_2Cu$	$C_{27}H_{19}N_5OSCu$	$C_{31}H_{20}N_4OS_2Cu$	$C_{31}H_{21}N_5OSCu$
Lattice constant	a ( $\text{\AA}$ )	10.536	12.172	11.38	23.20
	b ( $\text{\AA}$ )	9.706	14.012	16.63	17.58
	c ( $\text{\AA}$ )	12.791	15.901	10.82	16.34
Inter axial angle	$\alpha$ ( $^\circ$ )	90.000000	90.000000	90.000000	90.000000
	$\beta$ ( $^\circ$ )	111.96	91.26	90.000000	90.30
	$\gamma$ ( $^\circ$ )	90.000000	90.000000	90.000000	90.000000
Crystal system		$a \neq b \neq c$ , $\alpha = \gamma = 90$ , $\beta \neq 90$	$a \neq b \neq c$ , $\alpha = \gamma = 90$ , $\beta \neq 90$	$a \neq b \neq c$ , $\alpha = \beta = \gamma = 90$	$a \neq b \neq c$ , $\alpha = \gamma = 90$ , $\beta \neq 90$
		Monoclinic	Monoclinic	Orthorhombic	Rhombohedral
Unit cell Volume ( $\text{\AA}^3$ )		1213	2711	2047	6664
$2\theta$ range		11.594-45.74	11.614-79.48	10.577-55.22	10.612-52.28
Crystallite Size		133	649	192	747
Density ( $\text{g cm}^{-3}$ )		1.720	3.597	1.782	-

**Table 5:** Percentage cytotoxicity of the compounds at 100  $\mu$ M\*

Complex	A 549	Caco-2	HT-29	RPE-1
(3)	$68.6 \pm 6.5$	$98 \pm 0.05$	$71.3 \pm 0.5$	$71.6 \pm 5.7$
(4)	$99.8 \pm 0.3$	$99.9 \pm 0.05$	$94.5 \pm 0.7$	$99.3 \pm 2$
(5)	$72.5 \pm 4.5$	$28.7 \pm 12.2$	$87.9 \pm 0.7$	$55.6 \pm 5.1$
(6)	$89.6 \pm 1.5$	$96.6 \pm 1.9$	$98.6 \pm 0.2$	100
Dox	$0.31 \pm 0.019$	$4.22 \pm 0.33$	$2.75 \pm 0.15$	$8.9 \pm 2.1$

\*Results are calculated as average cytotoxicity  $\pm$  standard deviation

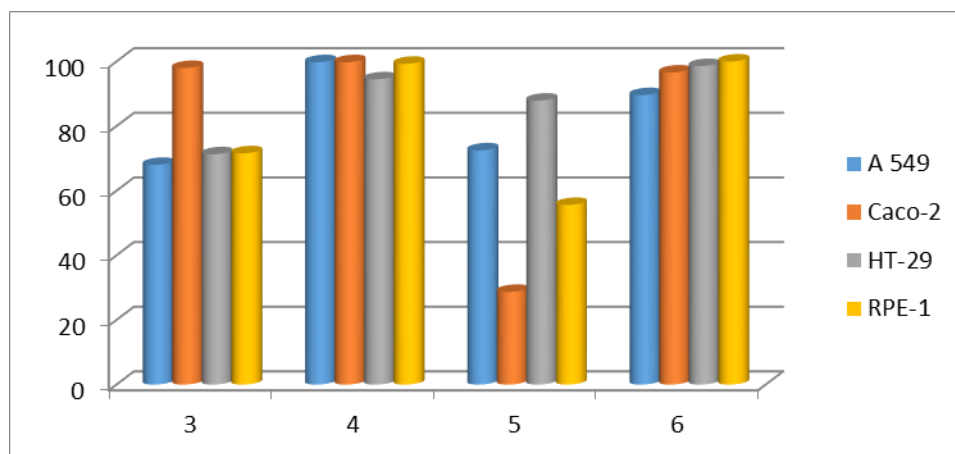


**Figure 5:** Percentage cytotoxicity of the compounds at 100  $\mu$ M

The half-maximal inhibitory concentration  $IC_{50}$  of the compounds, summarized in Table 6, manifests that the complex (5) present weak cytotoxicity against diverse human cell lines. Complex (3) presents a good activity on both A-549 and Caco-2 but with little selectivity. Complex (4) was highly active on both A-549 and Caco-2, with good selectivity on lung human cancer A-549 and moderate selectivity on colorectal cell line Caco-2.

**Table 6:** half maximal inhibitory concentration  $IC_{50}$  of the compounds in  $\mu M$

Complex	A-549	$r^2$	Caco-2	$r^2$	HT-29	$r^2$	RPE-1	$r^2$
(3)	27.7 ± 14	0.56	31 ± 5	0.94	65 ± 4	0.98	51.7 ± 7,	0.98
(4)	10.9 ± 2.5	0.81	15.7 ± 1,	0.98	30 ± 2	0.99	34.5 ± 2.6,	0.84
(5)	47.7 ± 15	0.78	166.6 ± 10	0.75	57.9 ± 11.5	0.84	92.6 ± 5.6,	0.96
(6)	12.4 ± 2	0.96	48 ± 1.5	0.99	23.7 ± 3.5	0.94	36.6 ± 1.7	0.90
Dox	0.2 ± 0.02	0.95	6 ± 1	0.99	0.9 ± 1	0.86	22.9 ± 13.9	0.85

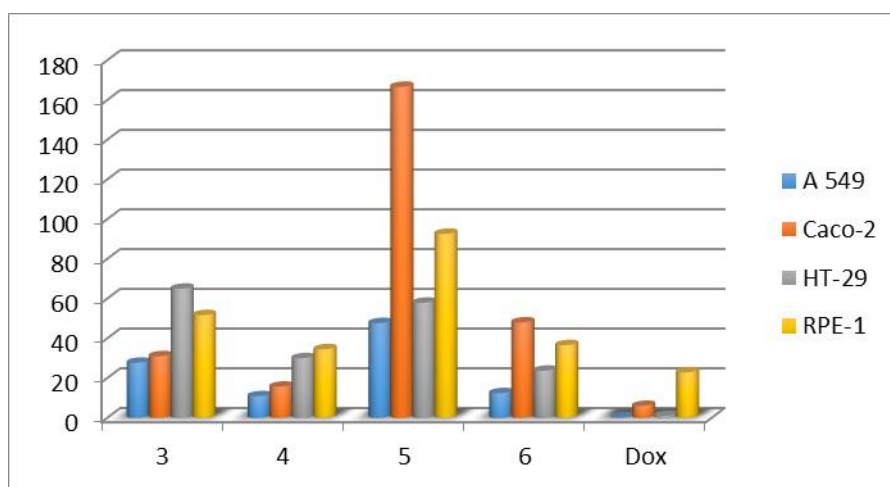


**Figure 6:** inhibitory concentration  $IC_{50}$  of the compounds in  $\mu M$

**Table 7:** Selectivity index ( $IC_{50}$  on cancer cell line /  $IC_{50}$  on normal cell line)

Complex	RPE-1/A-549	RPE-1/Caco-2	RPE-1/HT-29
(3)	1.8	1.66	0.79
(4)	3.1	2.19	1.15
(5)	1.94	0.55	1.59
(6)	2.95	0.76	1.5
Dox	2.5	3.7	25

## Conclusion

Novel mixed Complexes (3)-(6) was elaborated from two Schiff base ligand ((benzimidazol-2-phenyl)iminomethyl)phenol (HL1) (1) and 2-(1-H-benzimidazol-2-yl)phenyl)imino)methyl) naphthol (HL2) (2), copper salt ( $CuCl_2 \cdot 2H_2O$ ) and respectively 2-mercaptobenzothiazole or 2-aminobenzothiazole. The resulted data indicate that the copper is linked to ligands via deprotonated phenolic oxygen atom, nitrogen or sulphur atom of co-ligands and the coordination was realized through the azomethine group. X-ray powder diffraction analysis of complexes suggest that they possess monoclinic structure for complexes (3) and (4), while complex (5)

The best result was described with complex (6) and present highly active on lung human cancer A-549 with a very good selectivity versus its effect on the normal cell line. It was also active but not highly selective on HT-29. Therefore, complex (6) is a good candidate for further study on A-549 and complex (4) is a good candidate for further study on both A-549 and Caco-2 cell lines.

has orthorhombic structure and Rhombohedral structure for complex (6). The *in vitro* anticancer activities of the different complexes were evaluated and the results revealed an important cytotoxicity of complex (6) against lung human cancer A-549 and very good selectivity with 12.4 values of inhibitory concentration  $IC_{50}$ . The best result was described with complex (4) and present high activities on both A-549 and Caco-2 indicating good selectivity on lung human cancer A-549 and moderate selectivity on colorectal cell line Caco-2 with 10.9 and 15.7 respectively of  $IC_{50}$ .

## Declaration of competing interest:

The authors declare that they have no conflict of interest.

**Acknowledgment:**

The author(s) gratefully acknowledge Qassim University, represented by the Deanship of Scientific Research, on the material support for this research

**References**

1. Dokla E. M., Abutaleb N.S., Milik S.N., Li D., El-Baz K., Shalaby M.A., Al-Karaki R., Nasr M., Klein C.D., Abouzid K.A., Seleem M.N. Development of benzimidazole-based derivatives as antimicrobial agents and their synergistic effect with colistin against gram-negative bacteria. *Eur. J. med. Chem.*, **186**, 111850 (2020).
2. Tayade A. P., Pawar R. P. The Microwave Assisted and Efficient Synthesis of 2-Substituted Benzimidazole Mono-Condensation of *O*-Phenylenediamines and Aldehyde. *Polyc. Arom. Comp.*, 1-5 (2020)
3. Mavrova A. T., Anichina K. K., Vuchev D. I., Tsenov J. A., Denkova P. S., Kondeva M. S., Micheva M. K., Antihelminthic activity of some newly synthesized 5 (6)-(un) substituted-1H-benzimidazol-2-ylthioacetyl piperazine derivatives”, *Eur. J. Med. Chem.* **41**(12) 1412-20(2006).
4. Kuo H. L., Lien J. C., Chung C. H., Chang C. H., Lo S. C., Tsai I. C., Peng H. C., Kuo S. C., Huang T. F., NP-184 [2-(5-methyl-2-furyl) benzimidazole], a novel orally active antithrombotic agent with dual antiplatelet and anticoagulant activities. *Naunyn-Schmiedeberg's arch. Pharmacol.* **381**(6), 495-505 (2010).
5. Maghraby M.T., Abou-Ghadir O.M., Abdel-Moty S.G., Ali A.Y., Salem O.I. Novel class of benzimidazole-thiazole hybrids: The privileged scaffolds of potent anti-inflammatory activity with dual inhibition of cyclooxygenase and 15-lipoxygenase enzymes. *Bioorg. Med. Chem.* **28**, 115403-22 (2020).
6. Imran M., Al Kury, L.T., Nadeem H., Shah F.A., Abbas M., Naz S., Khan A.U., Li S. Benzimidazole Containing Acetamide Derivatives Attenuate Neuroinflammation and Oxidative Stress in Ethanol-Induced Neurodegeneration. *Biomolecules* **10**(1), 108-24 (2020)
7. Noor A., Qazi N.G., Nadeem H., Khan A.U., Paracha R.Z., Ali F., Saeed A. Synthesis, characterization, anti-ulcer action and molecular docking evaluation of novel benzimidazole-pyrazole hybrids. *Chem. Central J.* **11**(1), 85-98 (2017).
8. Khodja I.A., Boulebd H., Bensouici C., Belfaitah A. Design, synthesis, biological evaluation, molecular docking, DFT calculations and in silico ADME analysis of benzimidazole-hydrazone derivatives as promising antioxidant, antifungal, and anti-acetylcholinesterase agents. *Journal of Molecular Structure* **1218**, 128527 (2020).
9. Patel, V. M., Patel, N. B., Chan-Bacab, M. J., & Rivera, G. N-Mannich bases of benzimidazole as a potent antitubercular and antiprotozoal agents: Their synthesis and computational studies. *Synth. Commun.*, **50**(6), 858-878 (2020).
10. Azadbakht M., Davoodi A., Hosseinimehr S.J., Keighobadi M., Fakhar M., Valadan R., Faridnia R., Emami S., Azadbakht M., Bakhtiyari A. Tropolone alkaloids from *Colchicum kurdicum* (Bornm.) Stef.(Colchicaceae) as the potent novel antileishmanial compounds; purification, structure elucidation, antileishmanial activities and molecular docking studies. *Experimental Parasitology* **213**, 107902-12 (2020).
11. Bakhotmah D. A., Al-Ahmadi A. A. Design and Synthesis of Some New 3-Oxo/thioxo-1, 2, 4-triazolo [4, 3-a] benzimidazole Derivatives Bearing a 4-Tolyl Sulfonyl Moiety as Antimycobacterial Agents. *Poly. Arom. Comp.* **2019**, 1-13 ((2019).
12. Francesconi V., Cichero E., Schenone S., Naesens L., Tonelli M. Synthesis and Biological Evaluation of Novel (thio) semicarbazone-Based Benzimidazoles as Antiviral Agents against Human Respiratory Viruses. *Molecules* **25** (7) 1487-1508 (2020).
13. Pan T., He X., Chen B., Chen H., Geng G., Luo H., Zhang H., Bai C. Development of benzimidazole derivatives to inhibit HIV-1 replication through protecting APOBEC3G protein. *Eur. J. med. chem.* **95**, 500-13 (2015).
14. Wang Z., Deng X., Xiong R., Xiong S., Liu J., Cao X., Lei X., Chen Y., Zheng X., Tang G. Design, synthesis and biological evaluation of 3', 4', 5'-trimethoxy flavonoid benzimidazole derivatives as potential anti-tumor agents. *MedChemComm* **9**(2) 305-15 (2018).
15. Schmit D., Milewicz U., Boerneke M.A., Burley S., Walsworth K., Um J., Hecht D., Hermann T., Bergdahl B. M. Syntheses and Binding Testing of N1-Alkylamino-Substituted 2-Aminobenzimidazole Analogues Targeting the Hepatitis C Virus Internal Ribosome Entry Site. *Australian J. Chem.* **73**(3) 212-21(2020)
16. Serafini M., Torre E., Aprile S., Grosso E.D., Gesù A., Griglio A., Colombo G., Travelli C., Paiella S., damo A A., Orecchini E. Discovery of highly potent benzimidazole derivatives as

- indoleamine 2, 3-dioxygenase-1 (IDO1) inhibitors: from structure-based virtual screening to in vivo pharmacodynamic activity. *J. Med. Chem.* **63**(6),3047-65 (2020).
17. Marcus A. J., Iezhitsu I., Agarwal R., Vassiliev P., Spasov A., Zhukovskaya O., Anisimova V., Ismail N. M., Intraocular pressure-lowering effects of imidazo [1, 2-a]-and pyrimido [1, 2-a] benzimidazole compounds in rats with dexamethasone-induced ocular hypertension, *Eur. J. Pharm.* **850**, 75-78 (2019).
  18. Hue B.T., Nguyen P.H., De T.Q., Van Hieu M., Jo E., Van Tuan N., Thoa T.T., Anh L.D., Son N.H., Thanh D.D., Dupont-Rouzeyrol M. Benzimidazole Derivatives as Novel Zika Virus Inhibitors. *ChemMedChem* **15**, 1-2 (2020).
  19. Rahim F., Zaman K., Taha M., Ullah H., Ghufraan M., Wadood A., Rehman W., Uddin N., Shah S.A., Sajid M., Nawaz F. Synthesis, in vitro alpha-glucosidase inhibitory potential of benzimidazole bearing bis-Schiff bases and their molecular docking study. *Bioorg. Chem.* **94**, 103394(2020).
  20. Guzelj S., Gobec M., Urbančič D., Mlinarič-Raščan I., Corsini E., Jakopin Ž. Structural features and functional activities of benzimidazoles as NOD2 antagonists. *Eur. J. Med. Chem.* **190**, 112089. (2020).
  21. Taha, M., Mosaddik, A., Rahim, F., Ali, S., Ibrahim, M., Almandil, N. B. Synthesis, antiglycation and antioxidant potentials of benzimidazole derivatives. *J. King Saud University-Science*, **32**(1), 191-194 (2020).
  22. Sharma, M. C. QSAR studies of novel 1-(4-methoxyphenethyl)-1H-benzimidazole-5-carboxylic acid derivatives and their precursors as antileukaemic agents. *Journal of Taibah University for Science*, **10**(1), 122-130 (2016).
  23. Surineni, G., Gao, Y., Hussain, M., Liu, Z., Lu, Z., Chhotaray, C., Islam M. M., Hameed H. M. A., Zhang, T. Design, synthesis, and in vitro biological evaluation of novel benzimidazole tethered allylidenehydrazinylmethylthiazole derivatives as potent inhibitors of Mycobacterium tuberculosis. *MedChemComm*, **10**(1), 49-60(2019)
  24. Sivaramakarthykeyan, R., Iniyaval, S., Saravanan, V., Lim, W. M., Mai, C. W., Ramalingan, C. Molecular Hybrids Integrated with Benzimidazole and Pyrazole Structural Motifs: Design, Synthesis, Biological Evaluation, and Molecular Docking Studies. *ACS omega*, **5**(17), 10089-10098 (2020).
  25. Scott, F., Fala, A. M., Pennicott, L. E., Reuillon, T. D., Massirer, K. B., Elkins, J. M., Ward, S. E. Development of 2-(4-pyridyl)-benzimidazoles as PKN2 chemical tools to probe cancer. *Bioorg. Med. Chem. Lett.*, **30**(8), 12704(2020).
  26. Bansal, Y., Silakari, O. The therapeutic journey of benzimidazoles: a review. *Bioorg.med. chem.*, **20**(21), 6208-6236 (2012).
  27. Mahmood, K., Hashmi, W., Ismail, H., Mirza, B., Twamley, B., Akhter, Z., Rozas I., Baker, R. J. Synthesis, DNA binding and antibacterial activity of metal (II) complexes of a benzimidazole Schiff base. *Polyhedron*, **157**, 326-334(2019).
  28. Cota, I., Marturano, V., Tylkowski, B. Ln complexes as double faced agents: Study of antibacterial and antifungal activity. *Coord.Chem. Rev.*, **396**, 49-71(2019).
  29. Wang, X., Ling, N., Che, Q. T., Zhang, Y. W., Yang, H. X., Ruan, Y., Zhao, T. T. Synthesis, structure and biological properties of benzimidazole-based Cu (II)/Zn (II) complexes. *Inorg. Chem. Commun.*, **105**, 97-101. (2019).
  30. Bharti, N., Garza, M. G., Cruz-Vega, D. E., Castro-Garza, J., Saleem, K., Naqvi, F., Maurya M. R., Azam, A. Synthesis, characterization and antiamebic activity of benzimidazole derivatives and their vanadium and molybdenum complexes. *Bioorg. Med. Chem. Lett*, **12**(6), 869-871. (2002).
  31. Li, Y., Lu, L., Zhu, M., Wang, Q., Yuan, C., Xing, S., Fu X., Mei, Y. Potent inhibition of protein tyrosine phosphatases by copper complexes with multi-benzimidazole derivatives. *Biometals*, **24**(6), 993-1004 (2011).
  32. Toro, P., Klahn, A. H., Pradines, B., Lahoz, F., Pascual, A., Biot, C., Arancibia, R. Organometallic benzimidazoles: Synthesis, characterization and antimalarial activity. *Inorg. Chem. Commun.*, **35**, 126-129 (2013).
  33. Chhonker, Y. S., Veenu, B., Hasim, S. R., Kaushik, N., Kumar, D., Kumar, P. Synthesis and pharmacological evaluation of some new 2-phenyl benzimidazoles derivatives and their Schiff's bases. *E-journal of chemistry*, **6** (S1), S342-S346 (2009).
  34. Chhajed, S. S., Upasani, C. D. Synthesis and in-silico molecular docking simulation of 3-chloro-4-substituted-1-(2-(1H-benzimidazol-2-yl) phenyl)-azetidin-2-ones as novel analgesic anti-inflammatory agent. *Arabian J. Chem.*, **9**, S1779-S1785 (2016).
  35. Paul, A., Gupta, R. K., Dubey, M., Sharma, G., Koch, B., Hundal, G., Hundal M. S., Pandey, D. S. Potential apoptosis inducing agents based on a new benzimidazole schiff base ligand and its dicopper (II) complex. *RSC advances*, **4**(78), 41228-41236(2014).

36. Liu, H., Zhang, B., Tan, C., Liu, F., Cao, J., Tan, Y., Jiang, Y. Simultaneous bioimaging recognition of  $Al^{3+}$  and  $Cu^{2+}$  in living-cell, and further detection of  $F^{-}$  and  $S^{2-}$  by a simple fluorogenic benzimidazole-based chemosensor. *Talanta*, **161**, 309-319 (2016).
37. Kaur, N., Singh, J., Raj, P., Singh, N., Singh, H., Sharma, S. K., Kim D. Y., Kaur, N. ZnO decorated with organic nanoparticles based sensor for the ratiometric selective determination of mercury ions. *New J. Chem.*, **40**(2), 1529-1534.
38. Tang L., Cai M. A highly selective and sensitive fluorescent sensor for  $Cu^{2+}$  and its complex for successive sensing of cyanide via  $Cu^{2+}$  displacement approach *Sensors and actuators B: chemical* **173**,862-7(2012).
39. Paul, A., Anbu, S., Sharma, G., Kuznetsov, M. L., Koch, B., da Silva, M. F. C. G., Pombeiro, A. J. Synthesis, DNA binding, cellular DNA lesion and cytotoxicity of a series of new benzimidazole-based Schiff base copper (II) complexes. *Dalton Transactions*, **44**(46), 19983-19996 (2015).
40. Eisenhauer, E. A., ten Bokkel Huinink, W. W., Swenerton, K. D., Gianni, L., Myles, J., Van der Burg, M. E., Vermoken J. B., Bruser K. Colombo, N. European-Canadian randomized trial of paclitaxel in relapsed ovarian cancer: high-dose versus low-dose and long versus short infusion. *J. Clinical Oncology*, **12**(12), 2654-2666(1994).
41. Bissery, M. C., Nohynek, G., Sanderink, G. J., Lavelle, F. Docetaxel (Taxotere): a review of preclinical and clinical experience. Part I: Preclinical experience. *Anti-cancer drugs*, **6**(3), 339-55 (1995).
42. Hurwitz, H., Fehrenbacher, L., Novotny, W., Cartwright, T., Hainsworth, J., Heim, W., Berlin J., Baron, A., Griffing S. Holmgren E., Ferrara N., Fyfe G., Rogers B., Ross R., Kabbinavar, F.. Bevacizumab plus irinotecan, fluorouracil, and leucovorin for metastatic colorectal cancer. *New England j. med.*, **350**(23), 2335-2342 (2004)
43. Aroua L. M., Novel Mixed Complexes Derived from Benzoimidazolphenylethanamine and 4-(Benzoimidazol-2-yl)aniline: Synthesis, characterization, antibacterial evaluation and theoretical prediction of toxicity, *Asian J. of Chem.* **32**, 1266-72. (2020).
44. Al-Hakimi, A. N., Alminderej, F., Aroua, L., Alhag, S. K., Alfaifi, M. Y., Mahyoub, J. A., Elbehairi S. E. Alnafisah, A. S. Design, synthesis, characterization of zirconium (IV), cadmium (II) and iron (III) complexes derived from Schiff base 2-aminomethylbenzimidazole, 2-hydroxynaphthadehyde and evaluation of their biological activity. *Arabian J. Chem.*, **13**(10), 7378-7389 (2020).
45. Ghrab, S., Aroua, L., Mekni, N., Beji, M. Simple approach for the regioselective synthesis of a bis ( $\beta$ -aminoalcohol) derived from polyoxyethylene: first report of fast ring-opening of polyoxyethylene diglycidyl ethers with sodium amide. *Research on Chemical Intermediates*, **44**(5), 3537-3548. (2018).
46. Ghrab, S., Aroua, L., Beji, M. One-pot Three Component Synthesis of  $\omega$ -(oxathiolan-2-thion-5-yl)- $\alpha$ -oxazolidin-2-ones. *J. Heterocy. Chem.*, **54**(4), 2397-2404 (2017).
47. Alminderej F. M., Synthesis, Design and Biological Evaluation of Antibacterial Activity of Novel Mixed Metal Complexes Derived from Benzoimidazolphenylethanamine and 6-Amino-N,N-dimethyluracil, *Letf. Org. Chem.* **17**.
48. Aroua L. M., Synthesis and characterization of novel mixed complexes derived from 2-aminomethyl benzimidazole and 2-(1H-Benzimidazol-2-yl) aniline and theoretical prediction of toxicity, *Egyptian Journal of Chemistry, Egypt. J. Chem.* **63**(12), 4757-4767 (2020).
49. Stockert, J. C., Horobin, R. W., Colombo, L. L., Blázquez-Castro, A. Tetrazolium salts and formazan products in Cell Biology: Viability assessment, fluorescence imaging, and labeling perspectives. *Acta histochemica*, **120**(3), 159-167 (2018).
50. Da Luz, D. S., Da Silva, D. G., Souza, M. M., Giroldo, D., Martins, C. D. M. G. Efficiency of Neutral Red, Evans Blue and MTT to assess viability of the freshwater microalgae *D esmodesmus communis* and *P ediastrum boryanum*. *Phycological research*, **64**(1), 56-60 (2016).
51. Van Tonder, A., Joubert, A. M., Cromarty, A. D. Limitations of the 3-(4, 5-dimethylthiazol-2-yl)-2, 5-diphenyl-2H-tetrazolium bromide (MTT) assay when compared to three commonly used cell enumeration assays. *BMC research notes*, **8**(1), 1-10 (2015).
52. Mohan, S., Sundaraganesan, N., Mink, J. FTIR and Raman studies on benzimidazole. *Spectrochimica Acta Part A: Molecular Spectroscopy*, **47**(8), 1111-1115 (1991).
53. Sundaraganesan, N., Ilakiamani, S., Subramani, P., Joshua, B. D. Comparison of experimental and ab initio HF and DFT vibrational spectra of benzimidazole. *Spectrochimica Acta Part A: Molecular and Biom. Spectro.*, **67**(3-4), 628-635 (2007).

54. Ahmed, I. T. Synthesis and spectroscopic characterization of some divalent metal complexes derived from 1, 4-dibenzoylthiosemicarbazide and N-[2-(3-benzoylthioureido) ethyl] benzamide. *Phosphorus, Sulfur, and Silicon and the Related Elements*, **181**(2), 267-278 (2006).
55. Hazra, M., Dolai, T., Pandey, A., Dey, S. K., Patra, A. Synthesis and characterisation of copper (II) complexes with tridentate NNO functionalized ligand: Density function theory study, DNA binding mechanism, optical properties, and biological application. *Bioinorganic chemistry and applications*, (2014).
56. Kara, Y., Avar, B., Kayraldiz, A., Guzel, B., Kurtoglu, M. Synthesis and genotoxicity of Schiff base transition metal complexes. *Heteroatom Chemistry*, **22**(2), 119-130 (2011).
57. Joseph, J., & Mehta, B. H. Synthesis, characterization, and thermal analysis of transition metal complexes of polydentate ONO donor Schiff base ligand. *Russian J. Coord. Chem.*, **33**(2), 124-129 (2007).
58. Baranwal, B. P., Fatma, T., Varma, A. Synthesis, spectral and thermal characterization of nano-sized, oxo-centered, trinuclear carboxylate-bridged chromium (III) complexes of hydroxycarboxylic acids. *Journal of Molecular Structure*, **920**(1-3), 472-477 (2009).
59. Kolmas, J., Jaklewicz, A., Zima, A., Bućko, M., Paszkiewicz, Z., Lis, J., Ślósarczyk A. Kolodziejcki, W. Incorporation of carbonate and magnesium ions into synthetic hydroxyapatite: the effect on physicochemical properties. *Journal of Molecular Structure*, **987**(1-3), 40-50 (2011).